PROTON STRUCTURE FUNCTIONS AT HERA

Bruno Stella

(on behalf of H1 and ZEUS Collaborations)[1]

III Università degli Studi di Roma and INFN Sez. Roma 3 (Italy)
V. d. Vasca Navale 89 , I-00146 Roma (E-mail: bruno.stella@roma1.infn.it)

Abstract. The electron-proton collider HERA, like an electron-mycroscope, explores the structure of the proton down to 10^{-16} cm and up to the situation of very high parton densities. The proton energy was upgraded from 820 to 920 GeV in the Fall of '98 and the luminosity has also substantially improved, with another factor of 3 upgrade expected to follow this year.

Inclusive proton structure functions have been studied with incident e^+ and e^- of 27 GeV in the neutral (NC) and charged (CC) current interactions as functions of the squared four-momentum transfer, Q^2, and of the fractional proton momentum carried by partons, x. The structure function F_2, as well as the $\gamma - Z^0$ interference term xF_3, have been measured in a range of Q^2 and $1/x$ that extends by orders of magnitude that reached by fixed target experiments. The DGLAP evolution equations [1] allow for a perturbative NLO QCD fit of the measured non-perturbative structure functions in the available kinematic range: α_S and the gluon density at low x are fitted at the same time with good precision. The longitudinal structure function, F_L, can be determined within the DGLAP formalism.

With CC, the electroweak unification has been tested; at high x, a first flavour decomposition of the light quarks is achieved. The contribution to F_2 of the charm quark has been measured and results to be relevant. Bounds on the radius of quarks and on compositeness are derived from the data at the highest Q^2, $100 \leq Q^2 \leq 40,000\ GeV^2$.

1 INTRODUCTION

HERA is the 27.6 GeV electron - 920 GeV proton storage ring accelerator built by DESY (Hamburg) with a substantial contribution of other nations. The proton structure is explored in the colliding mode in two of the straight interaction sections by H1 and ZEUS experiments and in the fixed (polarised) target mode by polarised electron beam in a third section (by the experiment HERMES, wose results will not be reported here). After starting its operation at the end of '92, in 1994-'97 HERA has been operated with e^+'s and 820 GeV protons ($\sqrt{s} = 300$ GeV, s being the cms energy squared), accumulating a luminosity of $\approx 40 pb^{-1}$ per experiment. The proton energy has been upgraded to 920 GeV in '98 ($\sqrt{s} = 318$ GeV) and the machine has been operated first with e^-'s ($L \approx 15 pb^{-1}$ per experiment) and then with e^+'s ($L \approx 60 - 70 pb^{-1}$ per experiment). The rate of integrated luminosity has increased every year, achieving recently order of 100 pb^{-1} per year. The upgrade of the machine going on this year will provide an other factor 3 improvement.

[1]Invited paper at "International Symposium on Hadrons and Nuclei", Seoul, Feb. 20-22 '01.

H1 and ZEUS apparata are very general and have common features: a central tracking system in a uniform magnetic field (along the beam axis); a huge electromagnetic and hadronic calorimeter system (more detailed in the proton direction, due to the asymmetric momenta of the beams); instrumented iron for muon tracking; "forward" (at 0° respect to the outgoing proton) proton and neutron detectors and "backward" (at 180° respect to the outgoing proton) electron and photon taggers. Their sensitivities and performances are different enough: to be short, H1 has been optimised for leptons ($\sigma(E)/\sqrt{E} = 12\%$ for electrons, $\approx 50\%$ for hadrons) and ZEUS has a better resolution for hadronic calorimetry ($\sigma(E)/\sqrt{E} = 18\%$ for electrons and 35% for hadrons) .

HERA is a world unique colliding facility for probing the proton at very small distances ($\sim 10^{-16}$cm). The main diagram, the t-channel exchange of a highly virtual gauge boson (γ, Z neutral current, W charged current) in DIS, with the definition of the relevant kinematic variables, is depicted in Fig. 1: Q^2 is the squared 4-momentum transfer, x is the fraction of proton momentum carried by the struck quark, y is the inelasticity. In the quasi-two body kinematics, only two variables are independent: $Q^2 = xys$.

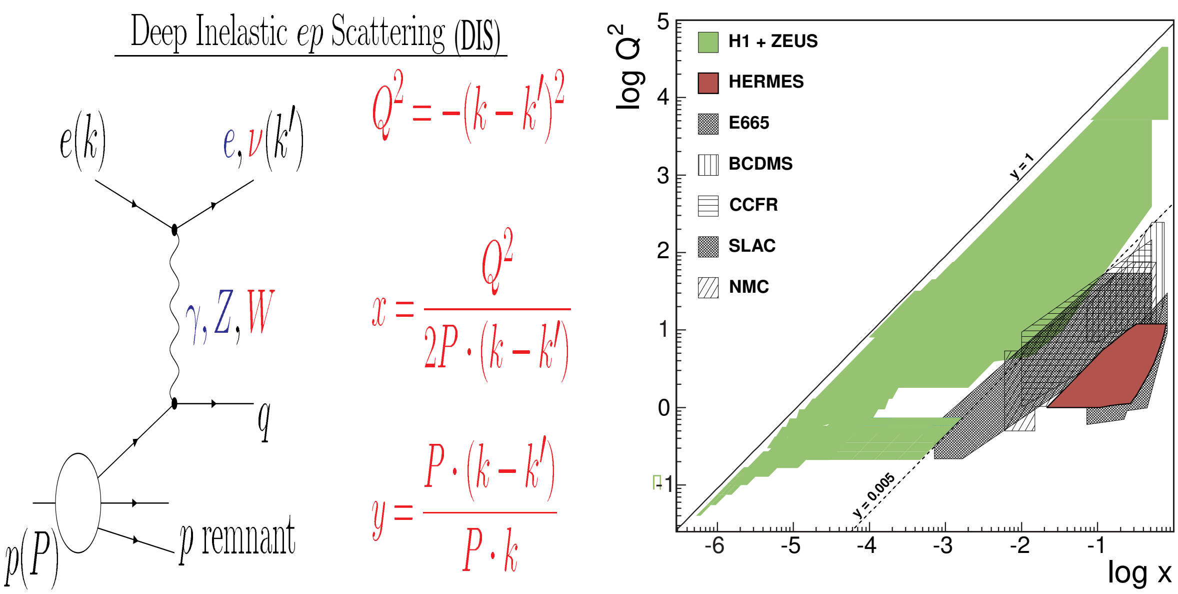

Figure 1: *(1a) Main diagram of DIS at HERA and definition of the kinematic variables. (1b) Q^2, x regions explored in various experiments, including fixed target ones.*

Fig. 1b shows the kinematic range (in logQ^2, log$x$) explored by HERA experiments (including HERMES) and by previous fixed target experiments; they overlap at small inelasticity (y$\sim$ 0.005). HERA has extended the explored range by almost three orders of magnitude, both in Q^2 and x.

QCD describes the proton as a dynamic fog of partons (quarks and gluons), u and d quarks at high fractional momentum x (valence quarks), irradiating gluons cascading in lower momentum gluons and quarks (sea quarks, of all possible flavours, including antiquarks) with degrading fractional momentum.

The high Q^2, high x limit (hard interactions) is the region of probing the proton at high resolution ($\equiv 1/\sqrt{Q^2_{max}}$), to check the pointlike nature of partons and their possible compositeness. The weak effects become sizable in NC , and EM and weak charged interactions give comparable cross sections for the first time. At lower x ($0.1 < x < 1.$) the quark densities can here be separated for the first time according to their flavour.

At very low x ($10^{-6} < x < 10^{-3}$), a region again explored for the first time by HERA, Q^2 is low (soft interactions), the parton density goes like a negative power of x and is than very high (gluons, sea quarks) and α_S is large; here the perturbative expansion of QCD (pQCD) is not valid anymore and the mechanism of confinement could be studied. Below $Q^2 \approx 1$ GeV^2 the physics is going to be hadronic (Regge limit) instead than partonic.

1.1 The neutral current cross section.

The "neutral current" events are identified inclusively by the presence in the final state of an high energy isolated electron, coplanar with the beam and the hadronic jet of the struck quark. An example of these NC events is shown in Fig. 2a with the ZEUS detector. They have very clear signatures: the proton remnant is visible in the proton (forward) direction , togeteher with a very energetic hadronic jet balanced in p_t (see transverse view) by the scattered electron.

The Born cross section for $e^{\pm}p \rightarrow e^{\pm}X$ is a linear combination of the "structure functions" F's:

$e^{\pm}p$: $(\frac{d^2\sigma^{NC}}{dxdQ^2})_{Born} = \frac{2\pi\alpha^2}{xQ^4}(Y_+F_2^{NC} \mp Y_- xF_3^{NC} - y^2F_L^{NC})$ with $Y_{\pm} = 1 \pm (1-y)^2$ (elicity term). By dividing by the coefficient, one gets the so called "reduced" cross section $\tilde{\sigma}$. xF_3 is the γ/Z interference term; $F_L(x, Q^2)$ is the longitudinal structure function, sensitive to gluons (it is zero with fermion partons only and at first order QCD).

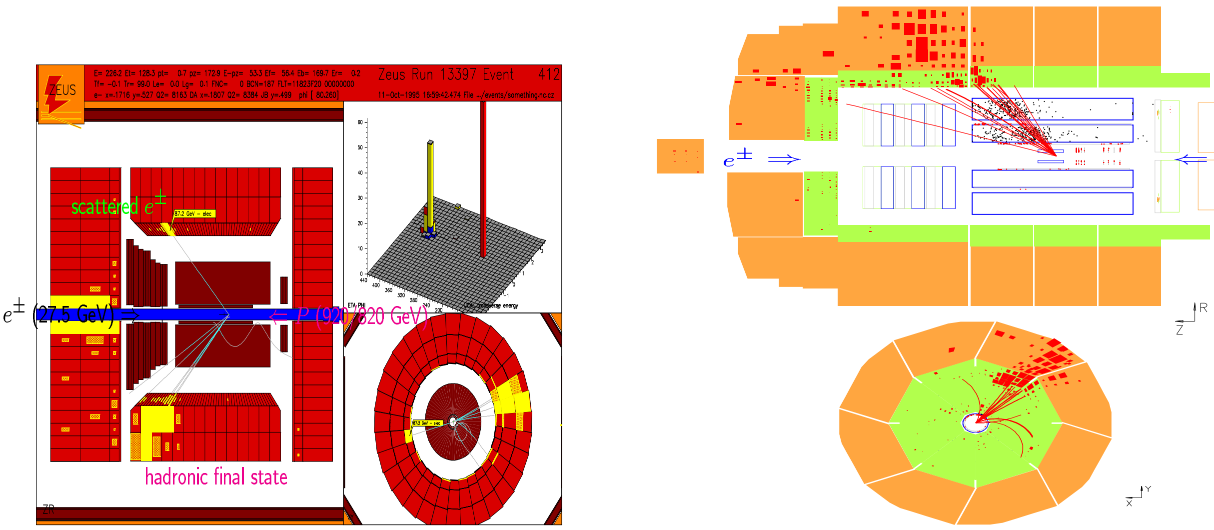

Figure 2: *(2a) A typical NC event detected by ZEUS experiment. (2b) A typical charged current event as detected by H1 (central detector). In both cases the projections along the beams and transverse to the beams are shown.*

In leading order QCD, the structure functions of x, Q^2 are combinations of the quark and antiquarks probability densities: $F_2(x, Q^2) = x\Sigma_{Quarks}A_f[q(x, Q^2) + \bar{q}(x, Q^2)]$. The coefficients A_{flavor} are the quark and anti-quark electric and weak charges (squared). The derivative $\frac{\delta F_2}{\delta log(Q^2)}$ is proportional to the gluon density $g(x, Q^2)$. The function

$xF_3(x,Q^2) = x\Sigma_{Quarks}B_f(q(x,Q^2) - \bar{q}(x,Q^2))$. The coefficients B_{flavor} are products of electric and weak charges of the different flavours.

1.2 The charged current cross section.

The charged current events ($e^{\pm}p \to \nu X$) have an undetected neutrino in the final state and are identified by a pure hadronic jet with high transverse momentum (together with remnants of the proton in the proton direction). A typical event is shown in Fig. 2b. In this case the recostruction is based on hadronic calorimeter data.

The CC cross section is suppressed at $Q^2 << M_W^2$ due to the high $W^{\pm}$ mass M_W: $\frac{d^2\sigma^{CC}}{dxdQ^2} = \frac{G_F^2}{2\pi x}\left(\frac{M_W^2}{Q^2+M_W^2}\right)^2 \cdot \tilde{\sigma}_{CC}^{\pm}$ $(\tilde{\sigma}_{CC}^{\pm} = Y_+F_2^{CC} \mp Y_-xF_3^{CC} - y^2F_L^{CC})$. The leading order cross sections are (for e^+ and e^-): $\tilde{\sigma}_{CC}^{e^+} = x \cdot [(\bar{u}+\bar{c}) + (1-y)^2(d+s)]$ (as valence quark, only d is probed, but is suppressed by the $(1-y)^2$ factor); $\tilde{\sigma}_{CC}^{e^-} = x \cdot [(u+c) + (1-y)^2(\bar{d}+\bar{s})]$ (as valence quark, only u is probed and is not suppressed). The two beams give important different informations with CC.

1.3 Outlook

In the following, in section 2, the proton structure is studied inclusively, both because the NC structure functions come out from the inclusive cross sections and because the proton is parameterised as an inclusive sum of partons. The data, analysed in the (non unique) framework of pQCD, as "evoluted" (functions of Q^2) according to DGLAP equations [1], give all the three structure functions, the gluon density and α_s. In section 3, CC cross sections are studied, with first evidence for the electroweak unification at high Q^2; the first attempts to measure flavour discriminated quark densities are reported, both for light (valence) quarks and for heavy quarks (charm). In section 4 the present limits for quark structure (quark radius, compositeness) are reported. A summary concludes the talk. [2]

2 INCLUSIVE PROTON STRUCTURE (NC).

The structure function F_2 is dominant at HERA for $Q^2 << M_Z^2$ and $y < 0.7$. At high x, by definition of "valence" only the three valence quarks are expected to contribute: the momentum of the three quarks would be statistically distributed, giving a gaussian distribution peaking at $x = 0.3$. At lower x, the structure function cannot be predicted by pQCD. The pre-HERA measurements (Fig. 3a) almost agreed with parton model, requiring little "sea quarks" contribution. Instead, as shown in Fig. 3a, the HERA experiments produced a structure function F_2 rising with decreasing x: the quark densities are rapidly increasing at low fractional momenta. This can be interpreted as due to gluon emission and subsequent splitting of the gluons into a quark-antiquark pair (or two gluons).

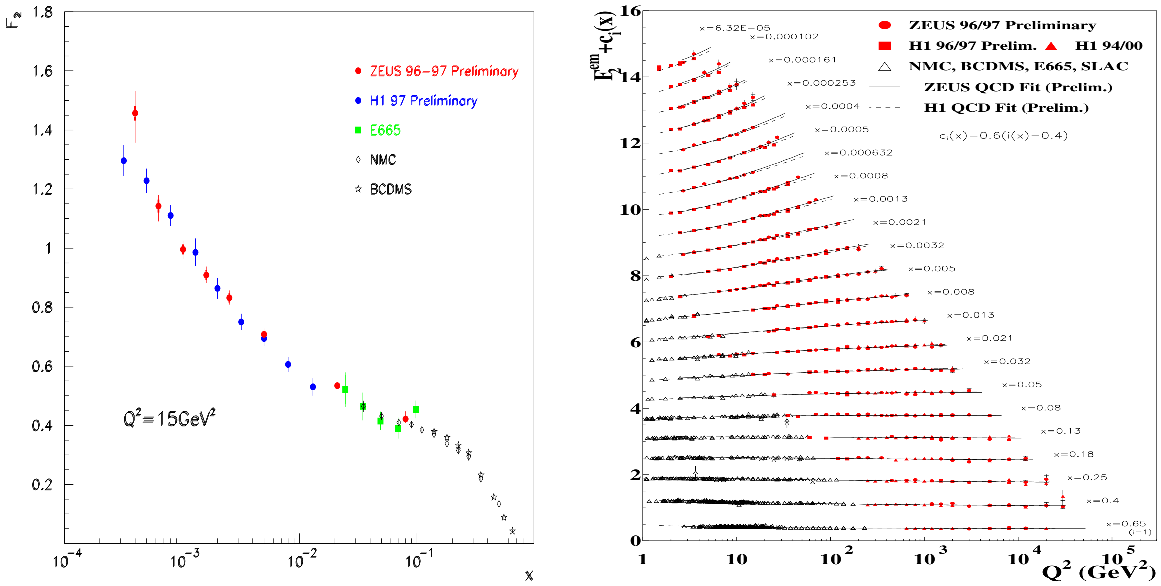

Figure 3: *(3a) The proton structure function* F_2 *as a function of* x *at* $Q^2 = 15$ *GeV*^{2} *(H1, ZEUS). (3b)* F_2 *as function of* Q^2*, for fixed* x*,* $3.2\ 10^{-5} < x < 0.85$.

2.1 Scaling violations of F_2 ('94-'97 data).

As function of Q^2, in the parton model F_2 is expected to stay constant because the quarks are considered to be pointlike and the photon can interact always with the same number of partons. In fact an almost constant F_2 had been observed by fixed target experiments (see in Fig. 3b the triangular points at low Q^2).

By extending very much the range in Q^2 and x, HERA experiments have evidentiated large scaling violations at low x (Fig. 3b, top lines) and also at high x (Fig. 4, bottom lines).

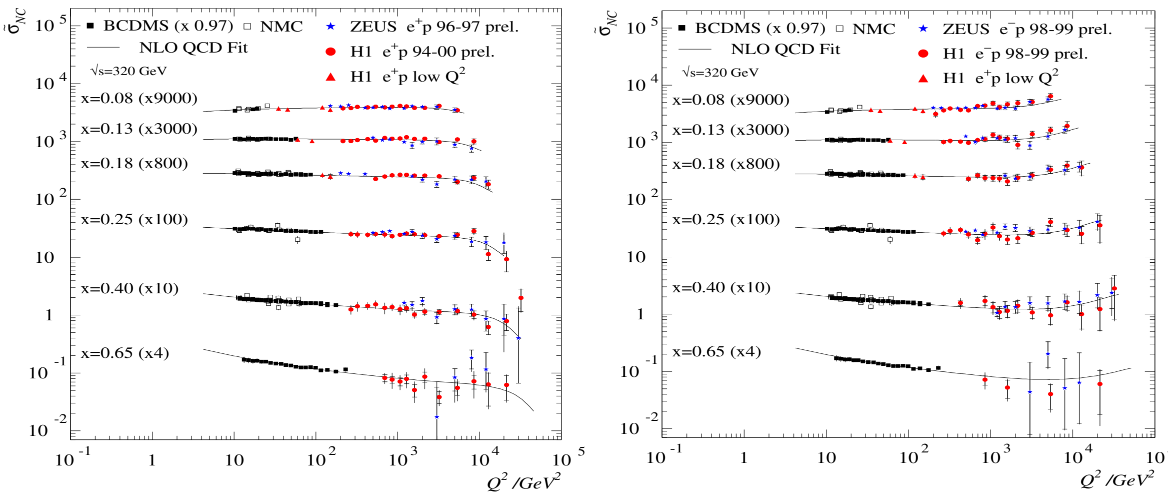

Figure 4: NC reduced cross section $\tilde{\sigma}_{NC}$ at high x, Q^2 (a test of the standard model (SM) over 4 orders of magnitude in Q^2; note the effect of the different sign of the γ/Z^0 interference in e^-(right) and e^+(left)).

It is remarkable that in the four (and more) decades of Q^2 explored by HERA the Q^2 dependence can be explained by gluon radiation by quarks (at high x) and quark emission by gluons (at low x), with a perfect description due to DGLAP evolution equations (see Next Leading Order (NLO) QCD fit lines in Fig.s 3b, 4). Moreover, not only ZEUS and H1 agree with each other, but also with the low Q^2 experiments.

2.2 Recent results at high Q^2 with e^-p and e^+p at $E_p = 920$ GeV ($\sqrt{s} = 318$ GeV)

After the machine upgrade in '98, with protons accelerated at 920 GeV, the comparison of the NC data with e^- and e^+ beam make now possible to test the Standard Model over 4 orders of magnitude in Q^2, including the small electroweak effects. The γ/Z interference is expected to be positive with e^- and negative with e^+. This is clearly visible experimentally in Fig. 4, where the reduced cross sections as function of Q^2 are presented, and Fig. 5 (the same as function of x) . Again the flat Q^2' and the steep $x$dependences are perfectly fitted by pQCD. [It must be said that the fit needs a large number (~ 25) of parameters, with technical choices; the choices and the parameters are not unique, even within the same evolution equations (DGLAP, [1]); other choices of evolution equations (CCFM, [3]) could reproduce as well the data at present]. The difference between e^- and e^+ is used to measure the interference term (next par.).

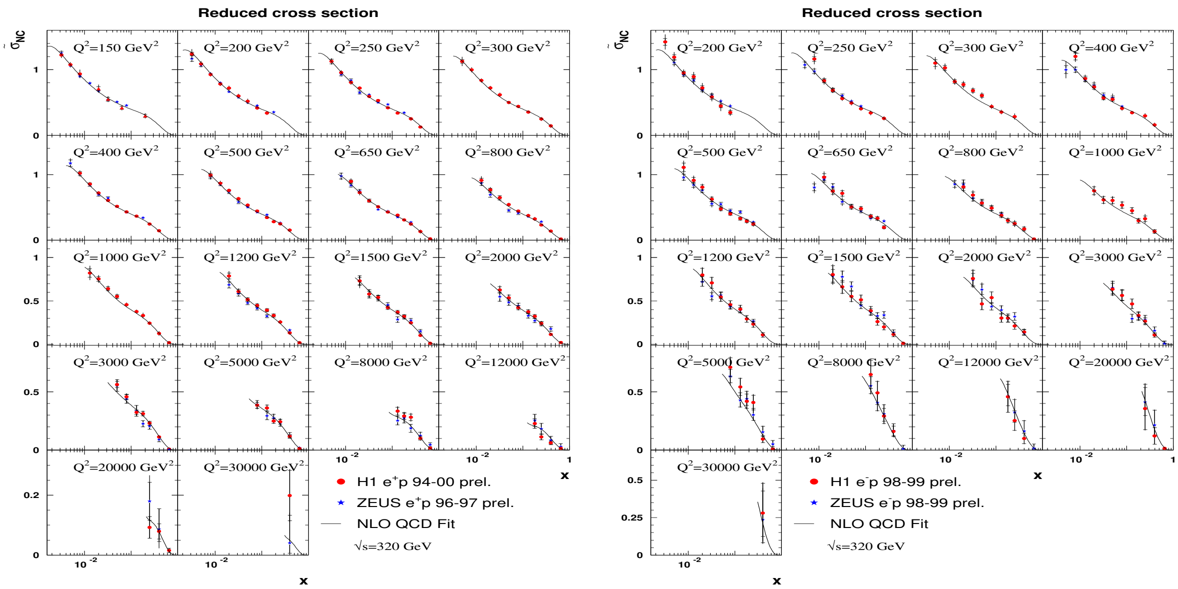

Figure 5: *NC reduced cross section $\tilde{\sigma}_{NC}$ for e^+ (left) and e^- (right): a stringent test of the pQCD + DGLAP (lines).*

2.3 Extraction of xF_3.

$\tilde{\sigma}^- - \tilde{\sigma}^+ = 2Y_- xF_3 = 2[1-(1-y)^2]xF_3$ (In case of different energies, kinematical corrections and F_L contributions are to be accounted for.) Fig. 6 shows the first measurements of xF_3. The preliminary results, for high $x$and high Q^2 (up to 30,000 GeV^2) compare well with the SM expectations.

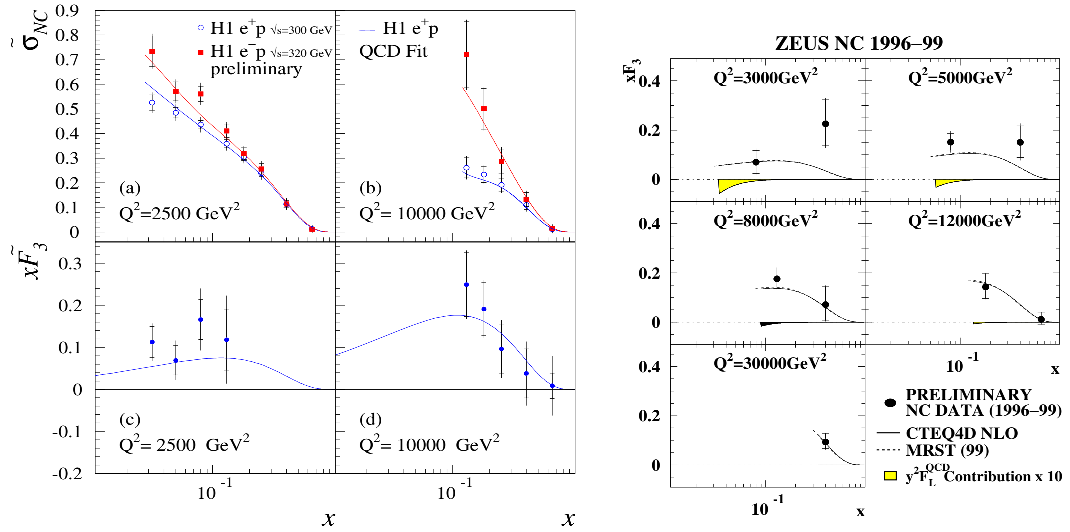

Figure 6: *First measurements of* xF_3^{NC} *at high* Q^2 *(sensitive to valence quark densities) by H1 (left) and ZEUS. [The* F_L *effect (*$\approx 1\%$*) is taken here from the QCD fit and lowest* x*]*

2.4 Determination of α_S and gluon density.

The most important parameters of pQCD are the coupling constant $\alpha_S(Q^2)$ and the gluon density g(x,Q^2). Up to now one of them was fixed by the world average and the other one was fitted. Now a simultaneous global fit is performed, which accounts for the anti-correlation of the two parametric functions. The results are shown in Fig. 7a (here in case of H1). The gluon density rises steeply at low $x$and high Q^2.

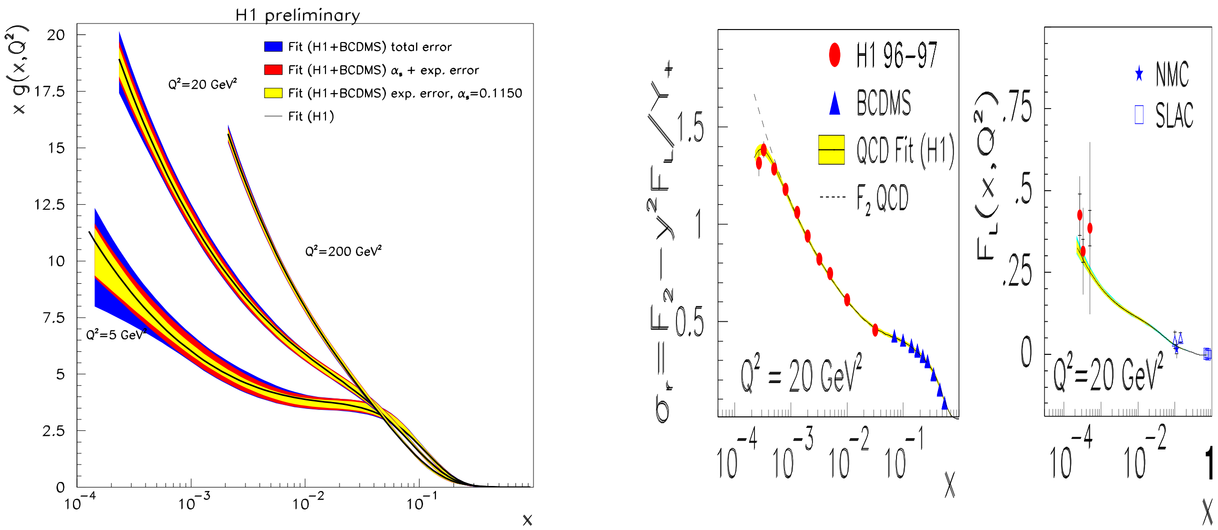

Figure 7: *(7a) Fit results on gluon density by H1. (7b) Extraction of* F_L *at low* x*; left:* $\tilde{\sigma}$ *(the dashed line corresponds to* $F_L = 0.$*), right: resulting* F_L*; both at* $Q^2 = 20 GeV^2$*.*

The corresponding α_S is: $\alpha_S(Z^0) = 0.1150 \pm 0.0017(exp) \pm 0.0012(model) \pm 0.005$ due to renormalisation scale uncertainty. Similar results are obtained by ZEUS. The values are in good agreement with the ones obtained from the DIS jet cross sections by the same experiments and with the world average, but show the running of α_S in a single experiment.

2.5 Longitudinal structure function F_L.

Assuming the validity of the pQCD theory used for the fit, the F_L structure function can be extracted. F_L shows up only at low x, when the partons are not only fermions, as a negative contribution to the cross section (see Fig. 7b). By subtracting $\tilde{\sigma}$ from F_2 (or by derivating $\tilde{\sigma}$ respect to y) H1 has got F_L within the DGLAP formalism (an example is shown in Fig. 7b), at x values 1000 times smaller than previous measurements.

2.6 Low Q^2, Low x: pQCD stops to work.

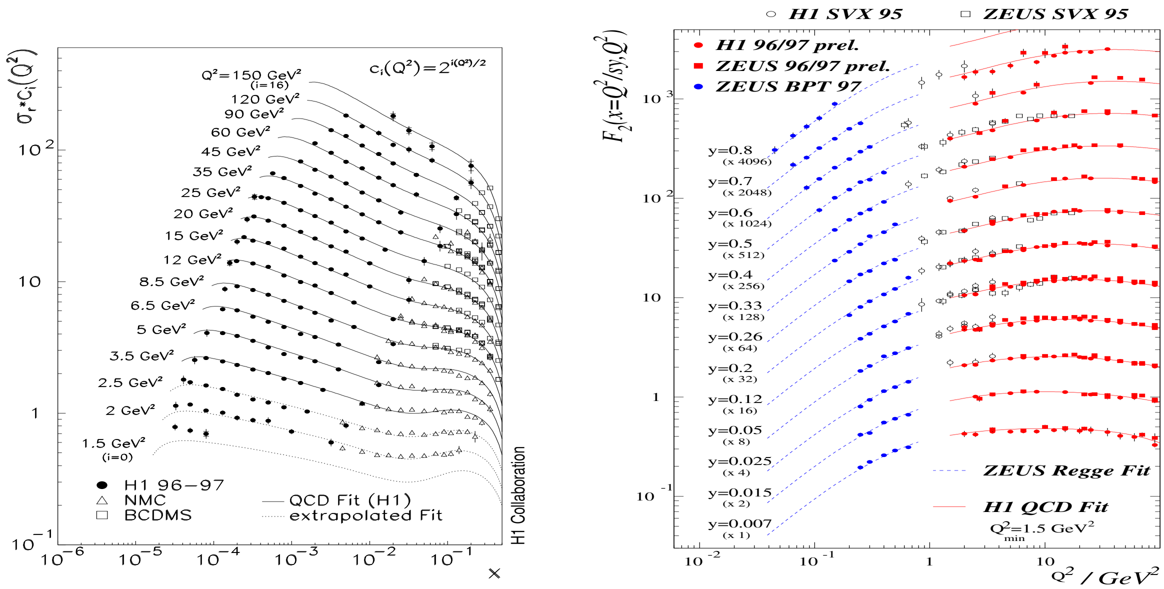

Figure 8: *(8a) Low Q^2, low x: behaviour of $\tilde{\sigma}$. (8b) F_2 at very low Q^2: hadronic $\leftrightarrow$ partonic junction.*

The pQCD fits could be performed technically even at very low Q^2, close to λ^2_{QCD}, when α_S^2 is not anymore much smaller than α_S; but they would loose theoretical meaning. This is why the fits must stop at some Q^2_{min} of the order of 1 GeV^2. Fig. 8a shows how nicely the fit describes the $x$dependence at various Q^2's, but stops to work at low $x$and low Q^2 (bottom lines).

At very low Q^2 we expect a transition between perturbative (partonic) and non-perturbative ($\equiv$ hadronic) QCD. This is experimentally evidentiated in Fig. 8b, where above $Q^2 \approx 1$ GeV^2 the H1 QCD fit is used to describe the data, and below $Q^2 \approx 1$ GeV^2, ZEUS data are well described by a fit inspired by Regge model. The approximate continuity between the two regimes is remarkable. Will we achieve a unified (partonic-hadronic) description of the proton structure function ?

3 CC and FLAVOUR DISCRIMINATED QUARK DENSITIES

3.1 CC differential cross section: testing the electro-weak sector (NC and CC, e^- and e^+).

The results for the CC cross section as function of Q^2 are shown in Fig. 9a. We see that HERA data agree with SM on wide Q^2 range. It is evident the different coupling of the exchanged W (differently charged in the e^- and e^+ cases) with partons of the proton.

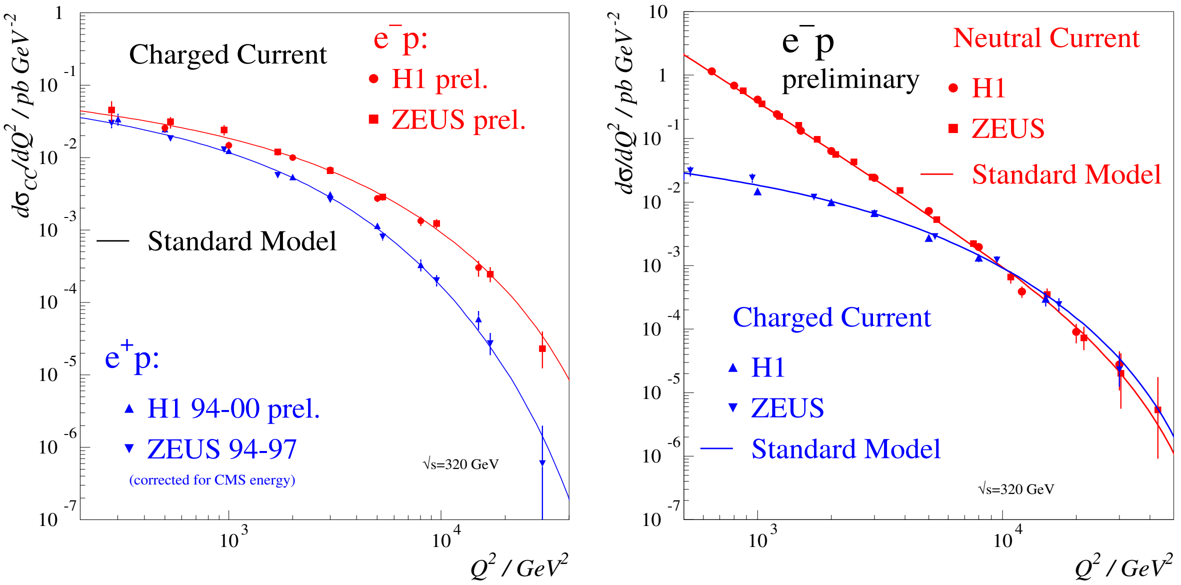

Figure 9: *(9a) CC cross section $d\sigma/dQ^2$ (e^- and e^+). (9b) Comparison of NC and CC cross section $d\sigma/dQ^2$ in case of e^-: electro-weak unification.*

If we compare NC (mostly electromagnetic) and CC (weak), we test that beyond $Q^2 \simeq M_W^2 \simeq M_Z^2$ the effect of the W propagator becomes small and the cross section are now similar. This is shown in Fig. 9b in case of e^-. So, we have encountered the electroweak unification !

3.2 Flavor specific parton density functions (PDF).

The NC structure functions are linear combinations of quark densities weighted with their (flavor specific) effective charges (squared). In case of CC, the different beam charges select (couple to) different combinations of flavors (as shown in the introduction). This can be used to measure the flavor discriminated PDF's.

3.3 Light quarks

At high x only the light quarks contribute to $\tilde{\sigma}_{NC}$ and $\tilde{\sigma}_{CC}$:
$\tilde{\sigma}_{NC}(e^+) \propto (1 + (1-y)^2)\Sigma e_f^2 x q_f$

$$\tilde{\sigma}_{CC}(e^+) \propto x\bar{u} + (1-y)^2 xd \quad ; \qquad \tilde{\sigma}_{CC}(e^-) \propto xu + (1-y)^2 x\bar{d}.$$

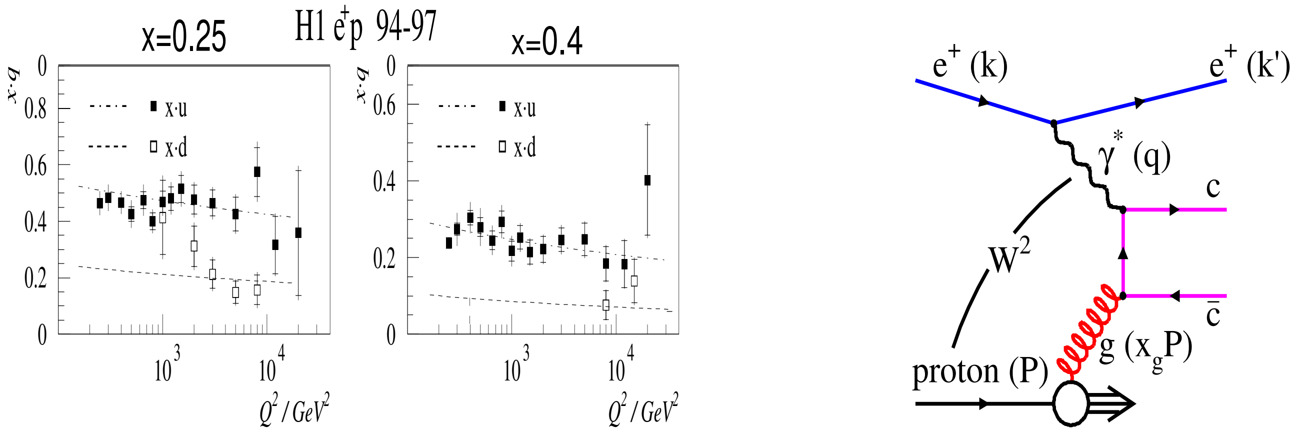

Figure 10: *(10a) Valence quark densities from high Q^2/high x, CC/NC (H1 e^+p data 94-97). (10b) Main charm-anticharm production diagram (boson-gluon fusion).*

H1 has used only the (high statistics) e^+ data to extract $u(x, Q^2)$ and $d(x, Q^2)$. The results at $x = 0.25$ and $x = 0.4$ are shown in Fig. 10a. The proton composition at high fractional momenta is here experimentally measured, without QCD inputs: u/d is slightly larger than 2. (More results have been presented at Osaka conference last year.) We don't have here the large uncertainties present in case of nuclei (fixed target experiments).

3.4 Heavy quark contribution to F_2.

Heavy quarks are produced in deep inelastic scattering mainly by the "boson-gluon fusion" process (Fig. 10b), which is sensitive to the gluon density in the proton. The diagram can also be interpreted as a probe to the charm (sea) quark content in the proton. The NC events are selected by requesting a $D^* \to K\pi\pi$ in the final state. The visible cross section has to be extrapolated to find the total one, by using xg(x) from QCD fit to inclusive F_2. ZEUS and H1 achieve good agreement in the $ep \to eD^*X$ cross section.

The $F_2^{\bar{c}c}(x, Q^2)$ results are shown in Fig. 11a. Again a strong rise towards low $x$is observed, as $F_2^{\bar{c}c} \propto xg(x)$. Fig. 11b presents the ratio $\frac{F_2^{\bar{c}c}}{F_2}$, as measured by ZEUS. It is evident that the charm content of the proton is non negligible, arriving even at 30% at high Q^2 and low x.

4 QUARK STRUCTURE

At high Q^2 the resolution is such that we might expect to probe the structure of the single quark in the proton.

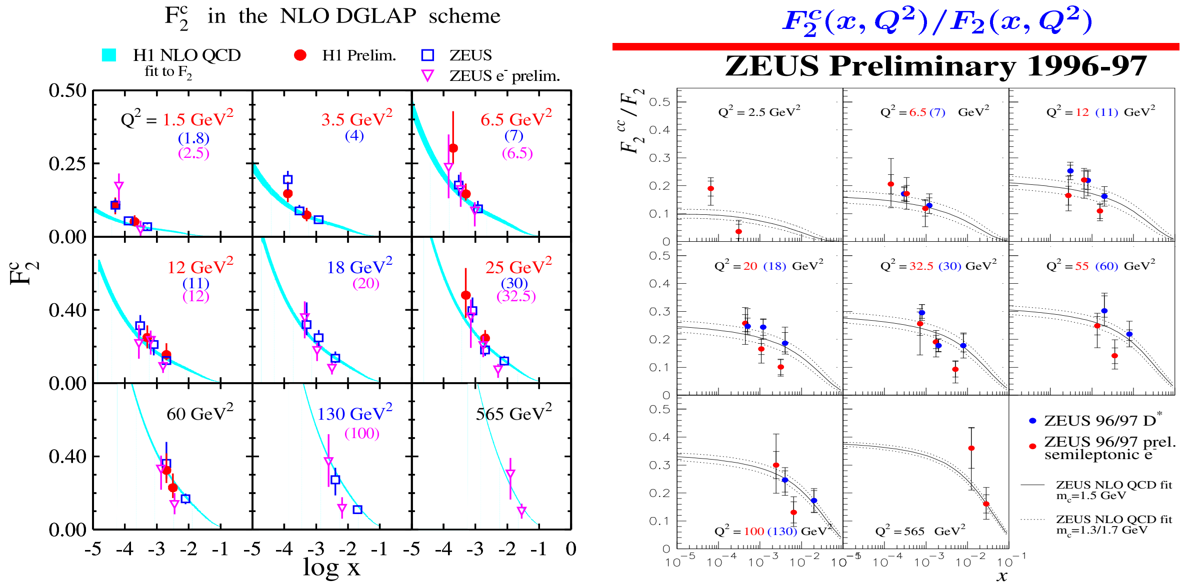

Figure 11: *Charm contribution to F_2 in the NLO DGLAP scheme: left, absolute; right, fractional.*

4.1 Quark radius

The simplest (over-simplified: static) interpretation of negative deviations from Q^2 spectrum at highest Q^2 is a spheric space charge distribution of the target quark. Parametrization of form factor of quarks: $f(Q^2) = 1 - 1/6 < R_q^2 > Q^2$ where R_q is the radius of the (uniform) quark charge distribution, to be fitted from the Q^2 dependence of the ratio of the experimental cross section with the SM expectation multiplied by the form factor. Fig. 12a shows the upper limits achieved by H1 with the low statistics e^-data and by ZEUS with the full available data.

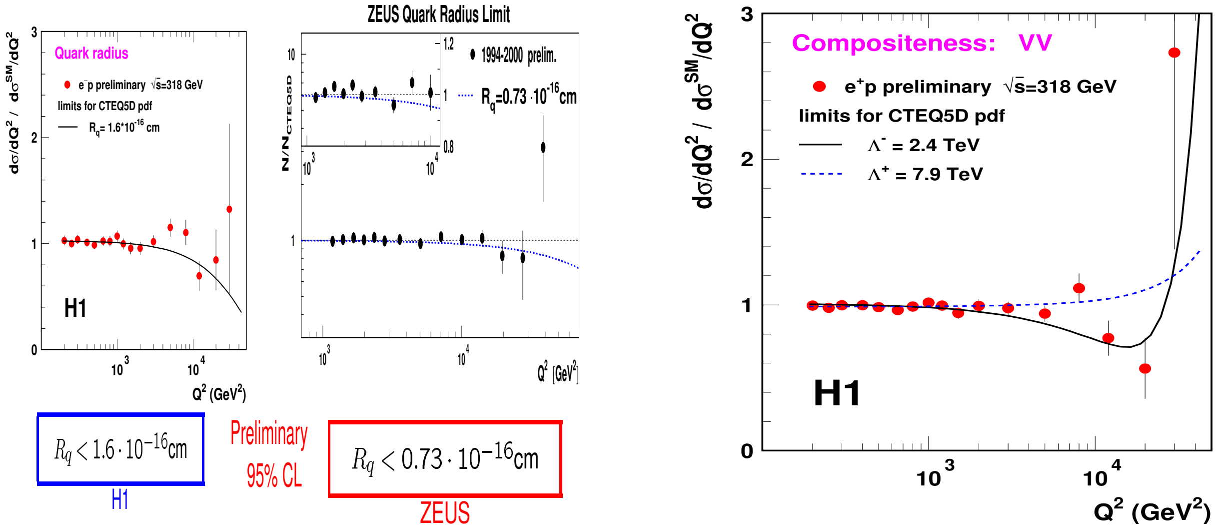

Figure 12: *(12a) Quark radius. Limits of H1 (e^-p data only) and ZEUS (global data). (12b) Fits on contact interaction models (VV case).*

HERA has then achieved a limit of 1/1000 of the proton radius for quarks. With only the valence quarks, the proton would then be almost empty, as the atom is!

4.2 Compositeness: contact interactions.

The structure of quarks can be studied in terms of compositeness by sub-elementary constituents, bound by a new interaction with caracteristic mass scale much larger than then the present center of mass scale: $\Lambda >> \sqrt{s}$. This can be parameterised as an effective 4 Fermion (eeqq) contact interaction with effective coupling $\eta^q_{ij} = \epsilon^q_{ij}(\frac{g}{\Lambda^q_{ij}})^2$ with i,j= left/right-handed particles (helicities); q= u,d quark flavors; $\epsilon^q_{ij} = \pm 1$: positive or negative interference with SM. Only vector coupling is assumed for HERA (scalar and tensor coupling terms are beyond the sensitivity of HERA). An example of the fits which give the lower limit of the coupling Λ is shown in Fig. 12b. The limits in both experiments achieve a few TeV in the various cases and are determined by the presence of fluctuations at the end of the Q^2 spectrum.

5 CONCLUSIONS

HERA experiments H1 and ZEUS have built up a wealth of new knowledge on structure functions and QCD in a very wide range of phase space ($0.11 < Q^2 < 46000\ GeV^2$; $\sim 10^{-6} < x < 0.7$). We have now at HERA all 4 double differential cross sections: NC, CC for e^+ and e^-. This enables us to extract special contributions for the first time, providing a sound phenomenological construction of strong interaction physics in the proton.

xF_3^{NC}, the $\gamma - Z^0$ term, has started to be measured at large Q^2. The Q^2 evolution equations named DGLAP allow for a NLO pQCD fit of the measured non-perturbative structure functions in the range $1 < Q^2 < 30,000$ GeV^2, $10^{-6} < x < 1$, with an impressive good description of the x, Q^2 behaviour. $xg(x, Q^2)$ and α_S have been fitted at the same time; the rapid rise of $g(x, Q^2)$ at low x has been confirmed and α_S has been measured with high precision.

The CC cross section shows the unification of electromagnetic and weak interactions at HERA energies. CC (alone and with NC) at high x allow for the measurement of flavour separated parton density functions (for valence quarks) with sensitivity to the d/u ratio, without nuclear corrections. The contribution of the charm quark to F_2 has been measured: it follows the $g(x, Q^2)$ rise at low x and is relevant (up to $\approx 30\%$). At the highest Q^2 the quark structure begins to be explored. The quark radius is measured to be smaller than 0.1% of the proton radius. Limits for compositeness (contact interactions) have been inproved.

HERA is facing a luminosity and detectors upgrade. In the years 2001-2005 HERA will have potential for significant and competitive improvements of existing limits on new phenomena (like leptoquarks, leptogluons, R_p-violating SUSY particles, excited electron, excited neutrino, contact interactions eeqq) and of course the opportunity to improve in details its precise measurements of the structure functions.-

References

[1] Yu. L. Dokshitzer, Sov. Phys, JETP 46 (1977) 641;
V.N. Gribov and L.N. Lipatov, Sov. J. Nucl. Phys. 15 ('72) 438 and 675;
G. Altarelli and G. Parisi, Nucl. Phys. B126 (1977) 298.

[2] Due to the lack of space, no detailed references can be given. The papers concerning the experimental results can be found in the WEB pages of the two experiments:
$http://www-zeus.desy.de/$
$http://www-h1.desy.de/h1/www/general/home/intra\_home.html$

[3] M. Ciafaloni, Nucl. Phys. B296 (1988) 49;
S. Catani, F. Fiorani and G. Marchesini, Nucl. Phys. B336 ('90) 18;
G. Marchesini, Nucl. Phys. B445 ('95) 45.